



PROF. MARC BRAMKAMP (Orcid ID : 0000-0002-7704-3266)

PROF. KIRSTEN JUNG (Orcid ID : 0000-0003-0779-6841)

Article type : Research Article

## **Elongation factor P is required for EII<sup>Glc</sup> translation in *Corynebacterium glutamicum* due to an essential polyproline motif**

**Bruno Pinheiro<sup>1</sup>, Dimitar Plamenov Petrov<sup>1</sup>, Lingyun Guo<sup>1</sup>, Gustavo Benevides Martins<sup>1</sup>, Marc Bramkamp<sup>2</sup>, Kirsten Jung<sup>1\*</sup>**

<sup>1</sup>Department of Biology I, Microbiology, Ludwig-Maximilians-Universität München, Martinsried, Germany.

<sup>2</sup>Institute for General Microbiology, Faculty of Mathematics and Natural Sciences, Christian-Albrechts-Universität zu Kiel, Kiel, Germany.

\*Corresponding author, jung@lmu.de

**Keywords:** *ptsG*; GntR2; EF-P; Translational control; Glucose uptake

### **HIGHLIGHTS**

EF-P is required for fast growth of *C. glutamicum* on glucose

EII<sup>Glc</sup> is subject to translational control

This article has been accepted for publication and undergone full peer review but has not been through the copyediting, typesetting, pagination and proofreading process, which may lead to differences between this version and the [Version of Record](#). Please cite this article as [doi: 10.1111/MMI.14618](https://doi.org/10.1111/MMI.14618)

This article is protected by copyright. All rights reserved

The polyproline motif in EII<sup>Glc</sup> is essential for its function

GntR2 also is EF-P dependent, but scarcely affects *ptsG* expression

#### CONFLICT OF INTEREST

The authors declare no conflict of interest.

#### SUMMARY

Translating ribosomes require elongation factor P (EF-P) to incorporate consecutive prolines (XPPX) into nascent peptide chains. The proteome of *Corynebacterium glutamicum* ATCC 13032 contains a total of 1,468 XPPX motifs, many of which are found in proteins involved in primary and secondary metabolism. We show here that synthesis of EII<sup>Glc</sup>, the glucose-specific permease of the phosphoenolpyruvate (PEP): sugar phosphotransferase system (PTS) encoded by *ptsG*, is strongly dependent on EF-P, as an *efp* deletion mutant grows poorly on glucose as sole carbon source. The amount of EII<sup>Glc</sup> is strongly reduced in this mutant, which consequently results in a lower rate of glucose uptake. Strikingly, the XPPX motif is essential for the activity of EII<sup>Glc</sup>, and substitution of the prolines leads to inactivation of the protein. Finally, translation of GntR2, a transcriptional activator of *ptsG*, is also dependent on EF-P. However, its

reduced amount in the *efp* mutant can be compensated for by other regulators. These results reveal for the first time a translational bottleneck involving production of the major glucose transporter EII<sup>glc</sup>, which has implications for future strain engineering strategies.

**Keywords:** *ptsG*; GntR2; Translational control; Glucose uptake; Phosphotransferase system

## INTRODUCTION

*Corynebacterium glutamicum* is an environmental bacterium whose natural ability to produce and secrete large amounts of L-glutamate and L-lysine is exploited for the industrial production of these amino acids (Heider and Wendisch, 2015, Becker et al., 2018, Sanchez et al., 2017, Eggeling and Bott, 2015). In addition, this bacterium has been engineered to produce plant-derived aromatic compounds (Kallscheuer et al., 2016, Kallscheuer et al., 2017), diamines (Meiswinkel et al., 2013, Peters-Wendisch et al., 2014), carotenoids (Peters-Wendisch et al., 2014, Henke et al., 2018), and biofuels (Siebert and Wendisch, 2015, Jojima et al., 2015, Xiao et al., 2016). As a facultative anaerobic chemoheterotroph, *C. glutamicum* utilizes a broad spectrum of carbohydrates as primary sources of both carbon and energy. Production strains are usually grown on feedstocks – such as molasses and starch or cellulose hydrolysates – containing either a complex mixture of sugars or consisting predominantly of glucose (Wendisch et al., 2016b, Wendisch et al., 2016a, Becker et al., 2018, Kallscheuer et al., 2019, Kogure and Inui, 2018). Therefore, the uptake and utilization of sugars, particularly glucose, are central elements of rational approaches to the engineering of high-performance production strains (Lindner et al., 2011, Martins et al., 2019, Hasegawa et al., 2017, Ikeda, 2012).

In *C. glutamicum*, carbohydrates like glucose, fructose and sucrose are taken up and phosphorylated by phosphoenolpyruvate (PEP)-dependent carbohydrate phosphotransferase systems (PTSs). Each PTS consists of two energy-coupling cytoplasmic proteins – the heat-stable phosphocarrier protein (HPr) and enzyme I (EI), which are common to all PTSs – and a set of sugar-specific enzyme II (EII) complexes located in the membrane. EII complexes are typically divided into three protein domains, EIIA, EIIB and EIIC, whose molecular organization differs between permeases and organisms. The variations involved range from examples in which all three domains are fused into one single protein – as is true of all PTS

permeases in *C. glutamicum* – to various combinations of fused and unfused domains (Gorke and Stulke, 2008, Deutscher et al., 2014) (Figure 1).

*C. glutamicum* is well known for its ability to co-metabolize different carbohydrates (Wendisch et al., 2000, Moon et al., 2007). However, the coordinated uptake of multiple substrates requires strict control of the expression and activity of the individual uptake systems. Transcriptional regulators, such as SugR, FruR, GntR1 and GntR2, form a complex network that up- and down-regulates the expression of sugar transporters and metabolic pathways according to sugar availability (Gaigalat et al., 2007, Engels and Wendisch, 2007, Tanaka et al., 2008a, Tanaka et al., 2008b, Frunzke et al., 2008, Tanaka et al., 2014). The *C. glutamicum* gene *ptsG* (Cgl1360, cg1537) encodes the glucose-specific, membrane-bound EIIBC component (EII<sup>Glc</sup>) responsible for the majority of glucose uptake (Moon et al., 2005, Moon et al., 2007) (Figure 1). In an attempt to increase glucose uptake and growth rates, transcription of *ptsG* has been placed under the control of inducible promoters. However, the higher mRNA levels were only very weakly reflected in EII<sup>Glc</sup> copy numbers or increased glucose uptake rates (Frunzke et al., 2008, Tanaka et al., 2008a, Krause et al., 2010, Wang et al., 2014, Lindner et al., 2013, Wang et al., 2018, Pfeifer et al., 2017). It was also shown that the presence of the corresponding sugars increases the size of PTS clusters within the membrane without significant increases in copy number (Martins et al., 2019). These observations suggested that other regulatory mechanism play a role in EII<sup>Glc</sup> production and glucose uptake capacity.

Ribosomes stall if certain polyproline motifs (XPPX) have to be incorporated into the polypeptide. In bacteria, elongation factor P (EF-P) has evolved to overcome this translational obstacle (Doerfel et al., 2013, Ude et al., 2013). EF-P orthologs with the same function, named aIF-5A and eIF-5A, exist in all archaea and eukaryotes, respectively (Gutierrez et al., 2013, Prunetti et al., 2016). For their activation, EF-P and its eIF5A/aIF5A orthologs usually require the post-translational modification of a conserved amino acid residue located at the tip of a loop (Roy et al., 2011, Yanagisawa et al., 2010, Peil et al., 2012, Lassak et al., 2015, Hummels et al., 2017). We recently demonstrated that the EF-Ps of Actinobacteria – specifically, *C. glutamicum*, *Streptomyces coelicolor* and *Mycobacterium tuberculosis* – alleviate ribosome stalling at polyproline motifs without the need for any activating post-translational modification (Pinheiro et al., 2020). In *C. glutamicum*, EF-P is required for the synthesis of many polyproline-containing enzymes of primary and secondary metabolism, as well as regulatory proteins (Pinheiro et al., 2020). Various studies have shown that polyproline motifs can play important functional roles in the catalytic center of enzymes, in the down-regulation of the copy numbers of receptors, and in protein-protein interactions (Motz and Jung, 2018, Ude et al., 2013, Starosta et al., 2014b). These motifs might also be important in protein folding and membrane insertion (Qi et al., 2018).

Here, we report that the translation of EII<sup>Glc</sup> in *C. glutamicum* is strongly dependent on EF-P, due to the presence of an essential polyproline motif at position 235/236. In a  $\Delta efp$  mutant, very little EII<sup>Glc</sup> is produced and glucose uptake is correspondingly reduced, thus essentially preventing the growth of cells on glucose as sole carbon source. These findings underline the fact that the translational level also needs to be considered in strain engineering.

## RESULTS

### Elongation factor P is required for fast growth of *C. glutamicum* on glucose

Although virtually all diproline-containing motifs cause translational stalling, the duration of stalling is modulated by the amino acids located upstream and downstream of the arrest motif. Therefore, polyproline motifs can be classified as weak, moderate or strong according to their ability to trigger ribosome stalling (Hersch et al., 2013, Elgamal et al., 2014, Starosta et al., 2014a, Woolstenhulme et al., 2015). This classification takes into consideration the translation initiation rate, the position of the motif within the peptide chain, and most importantly, the amino acid context up- (-2 and -1) and downstream (+1) of the diproline sequence itself. Evidence that there is also a hierarchy of pausing motifs in *C. glutamicum* originates from our previous proteome study in which the  $\Delta efp$  mutant was compared with the parental wild type strain (Pinheiro et al., 2020). We analyzed the amino acid sequences of the main proteins responsible for carbohydrate uptake, metabolism and transcriptional regulation in *C. glutamicum* ATCC 13032 (Figure 1, Table 1). Among these sequences, strong stalling motifs were found in EII<sup>Glc</sup>, the permease of the glucose PTS, and GntR2, a global transcriptional regulator which, among other genes, stimulates the transcription of *ptsG* (Frunzke et al., 2008, Tanaka et al., 2014, Ikeda, 2012) (Figure 1, Table 1). Weak XPPX stalling motifs were found in EII<sup>Fru</sup>, PfkB, EII<sup>Scr</sup>, ScrB, GntP and FruR (Figure 1).

To test whether EF-P is required for carbohydrate uptake and metabolism, we grew cells of the wild type and the *efp* deletion mutant in defined minimal medium in the presence of glucose, fructose, sucrose or ribose as a sole carbon source. We observed major growth defect of the  $\Delta efp$  mutant in a medium containing glucose as sole C-source (Figure 2E). The mutant exhibited slightly growth impairment relative to the wild type when grown on ribose, gluconate, fructose or sucrose as sole carbon source (Figure 2). Therefore, the severity of the growth defect correlates well with the expected stalling efficacies of the polyproline motifs observed in these transporters. After providing the *efp* gene *in trans*, growth of the

mutant was indistinguishable from wild type under all conditions (Figure 2, gray symbols). As a further control, the *efp* mutant was grown in rich BHI medium, and no growth defect was observed (Figure 2F).

### **EF-P is required for translation of EII<sup>Glc</sup>**

EII<sup>Glc</sup> has the strongest stalling XPPX motif found in any of the carbohydrate transporters identified in *C. glutamicum*. It was previously shown that fusion of the fluorescent mNeonGreen protein to the N-terminus of EII<sup>Glc</sup> (mNG-EII<sup>Glc</sup>) has no detectable effect on the transporter's function (Martins et al., 2019). To investigate the impact of EF-P on the production of the transporter, we analyzed the fluorescence of cells expressing this chromosomally encoded mNG-EII<sup>Glc</sup> hybrid in *efp*<sup>+</sup> and *efp*<sup>-</sup> genetic backgrounds. The overall fluorescence of the *efp*<sup>-</sup> cells was significantly lower than that of the *efp*<sup>+</sup> control (Figure 3A and 3B). In addition, many of the *efp*<sup>-</sup> cells showed fluorescence values in the range of the background fluorescence of untagged *C. glutamicum* ATCC 13032 indicating that mNG-EII<sup>Glc</sup> production was strongly reduced in the mutant (Figure 3A and 3B). It should be noted that the foci in these cells are polyphosphate granules, which are well known when *C. glutamicum* is imaged at 488 nm excitation (Martins et al., 2019).

The positive effect of EF-P on EII<sup>Glc</sup> synthesis could also be demonstrated *in vitro*. In this experiment, we used an *in vitro* transcription-translation system [PURExpress (NEB), with the modifications described in Experimental Procedures] and monitored the production of EII<sup>Glc</sup> over time, in the presence or absence of purified EF-P. We used a reporter DNA sequence encoding a double Flag-tagged EII<sup>Glc</sup> (FT-*ptsG*-FT), which allowed us to quantify the protein on Western blots using anti-Flag-Tag antibodies. In the presence of purified EF-P, the EII<sup>Glc</sup> translation rate was 2.3-fold faster than the control value without EF-P (Figure 3C).

We then tested whether the lower EII<sup>Glc</sup> amount in the *C. glutamicum*  $\Delta$ *efp* mutant affects the rate of glucose uptake. The kinetics of EII<sup>Glc</sup>-mediated uptake of radiolabeled D-glucose-6-<sup>14</sup>C were described previously, and yielded a  $K_m$  of 14  $\mu$ M and a  $V_{max}$  of  $35 \pm 3$  nmol min<sup>-1</sup> mg<sup>-1</sup> DW (Lindner et al., 2011). Under the same conditions, we obtained similar glucose uptake rates for the wild type however, the uptake rate of the  $\Delta$ *efp* mutant was significantly lower (Figure 3D). At saturating glucose concentrations, the uptake rate was determined to be  $38 \pm 4$  nmol min<sup>-1</sup> mg<sup>-1</sup> DW for the wild type and  $25 \pm 4$  nmol min<sup>-1</sup> mg<sup>-1</sup> DW for the  $\Delta$ *efp* mutant. As a negative control, we measured a glucose uptake rate of  $0.07 \pm 0.09$  nmol min<sup>-1</sup> mg<sup>-1</sup> DW for the  $\Delta$ *ptsG* mutant. Taken together, these results reveal that the  $\Delta$ *efp* mutant is still able to take up glucose, albeit at a markedly reduced rate, in agreement with the significantly reduced amount of the permease.

## Importance of the polyproline motif for EII<sup>Glc</sup> function

The requirement of EF-P for the translation of EII<sup>Glc</sup> raises the question on the function of the polyproline motif in this protein, because XPPX motifs are required for copy number regulation or dimerization or catalytic activity (Ude et al., 2013, Hummels and Kearns, 2019; Starosta et al., 2014b, Motz and Jung, 2018). To answer this question, we substituted alanines for the prolines at positions 235 and 236, and the corresponding construct *mNG-ptsG-PP235/236AA* was inserted into the native locus in *C. glutamicum*. Although this mutant grew at essentially the same rate as the wild type in the rich medium BHI (Figure 4A), it was unable to grow on glucose as the only carbon source (Figure 4B). The replacement of only one of the prolines by alanine in EII<sup>Glc</sup> (*mNG-ptsG-P236A*) also resulted in a non-functional transporter (Figure 4B), as the amino-acid replacements did not affect the synthesis of the protein (see Figure 4C). We then used primers containing wobble codons for semi-random mutagenesis to construct a *ptsG* library in which the proline codons are replaced by random amino acid codons. We sequenced several of the resulting clones, which confirmed the diversity of sequences generated (Figure 4D). Nevertheless, the introduction of the *ptsG* variant library into the  $\Delta ptsG \Delta iolT1 \Delta iolT2$  strain allowed growth on glucose only when the wild-type sequence was expressed (Brühl, 2015). It is important to mention here that IolT1 and IolT2 are two inositol permeases that can function as glucose transporter and are able to suppress the growth retardation in the absence of glucose-PTS system (Lindner et al., 2011, Ikeda et al., 2011). Therefore, the additional deletions in *iolT1* and *iolT2* were introduced into the  $\Delta ptsG$  mutant of *C. glutamicum* to avoid formation of unwanted second-site suppressor mutations. Our finding suggests that the XPPX-motif is important for the enzyme's function.

The XPPX motif is located in the EIIC domain of the protein, which is responsible for the translocation of the carbohydrate (Figure 1). Although the members of the EIIC glucose superfamily have low sequence identity, they are characterized by identical topologies (Nguyen et al., 2006, McCoy et al., 2016). The 3D-structure of the EIIC component of the maltose-specific PTS component MalT from *Bacillus cereus* was previously solved (PDB 5IW5) (McCoy et al., 2016). Use of *B. cereus* MalT to predict the structure of *C. glutamicum* EII<sup>Glc</sup> placed the XXPPX motif in a transmembrane domain that is involved in the dimerization of the PTS component (Figure 4E). In addition, the sequence of *C. glutamicum* EIIC<sup>Glc</sup> was used to identify and collect similar amino acid sequences. Of the 4,219 non-redundant sequences, 14.6% have XPPX motifs, including the EIIC sequences of *E. coli*, *Vibrio natriegens*, *Staphylococcus epidermidis*, *Klebsiella oxytoca* and their translation might as well depend on EF-P (Figure 4F). It is important to note that the amino acids up- and downstream of the polyproline motifs also differ between the sequences, which on

the one hand is consistent with the low amino acid sequence conservation in the EIICs of the glucose superfamily, but on other hand influences the stalling strength (Elgamal et al., 2014; Starosta et al., 2014a, Woolstenhulme et al., 2015).

### **The dependency of GntR2 translation on EF-P does not affect the transcription of *ptsG***

Although EF-P acts only at the translational level, it might indirectly influence the transcription of certain genes by affecting the translation of transcriptional regulators. Among the network of transcriptional regulators of *ptsG* identified so far, GntR2 contains a XPPX stalling motif. GntR2 is a global transcriptional regulator of the GntR-type that simultaneously activates *ptsG* and *ptsS* expression, strongly represses *gntP* and *gntK*, and weakly represses transcription of genes coding for enzymes of the pentose phosphate pathway (Frunzke et al., 2008, Tanaka et al., 2014). Owing to the presence of this XPPX motif, we wondered whether EF-P regulates the copy number of GntR2 and consequently the *ptsG* expression. To address this question, we fused the *gntR2* gene to a sequence encoding the fluorescent protein mCherry (C-terminal), and inserted this construct into the native locus in *C. glutamicum*. Then we quantified the fluorescence of GntR2-mCherry in both *efp*<sup>+</sup> and *efp*<sup>-</sup> strains (Figure 5A and 5B). The GntR2-mCherry level was 4.8 times lower in the *efp*<sup>-</sup> strain, confirming the dependency on EF-P. However, transcription of *ptsG* was not detectably altered in the *efp*<sup>-</sup> strain (Figure 5C). The lack of an effect of the *efp* deletion could be related to the presence of two GntR-like regulators (GntR1 and GntR2) with redundant functions in *C. glutamicum* ATCC 13032. Only when both genes are deleted, growth defects are observed in glucose-containing medium, while each of the  $\Delta gntR1$  or  $\Delta gntR2$  mutants behaves like the wild type (Frunzke et al., 2008).

## **DISCUSSION**

EII<sup>Glc</sup> is the major glucose transporter in *C. glutamicum*. Increasing the expression of *ptsG*, which codes for the glucose transporter, is a commonly used strategy to increase the glucose consumption rate in order to boost the production of amino acids and secondary metabolites (Lindner et al., 2013, Krause et al., 2010, Xu et al., 2016). However, so far, the logarithmic increases in *ptsG* transcription levels caused by inducible promoters have been followed by only a small increase in EII<sup>Glc</sup> copy number and/or glucose uptake rate (Wang et al., 2018, Krause et al., 2010, Wang et al., 2014, Lindner et al., 2013). In this study, we

demonstrate through a combination of bioinformatic analysis and phenotypic characterization of a *C. glutamicum* *efp* deletion mutant that EF-P is 456 required for the translation of this carbohydrate transporter. *In vivo*, the deletion of *efp* resulted in a decrease in the content of EII<sup>Glc</sup>, lower glucose uptake rates, and impaired growth of cells on glucose as carbon source. The direct effect of purified EF-P on the translation of EII<sup>Glc</sup> was confirmed *in vitro*. Interestingly, the transcription of *ptsG* was not affected in the *efp* mutant, although it turned out that one of its transcription activators GntR2 was dependent on EF-P. The fact that the reduction in the copy number of GntR2 in the *efp* mutant had little or no impact on *ptsG* transcription, could be explained by compensation by other regulators in *C. glutamicum* ATCC 13032 make up for its loss (Frunzke et al., 2008). These results indicate that regulation of *ptsG* expression is rather robust, whereas translation is impeded by periods of stalling, which can be alleviated by the activity of EF-P. This translational regulation might serve to prevent the overproduction of EII<sup>Glc</sup> molecules, thus protecting *C. glutamicum* from the so-called phosphosugar stress (Lindner et al., 2013). In *E. coli* protection against phosphosugar stress is provided by a complex regulatory network involving small RNA-initiated inhibition of *ptsG* translation, and Hfq-dependent *ptsG* mRNA degradation by RNase E (Maki et al., 2008, Morita et al., 2005). *C. glutamicum* does not possess an Hfq homolog (Kalinowski et al., 2003) and therefore, might use the polyproline-dependent stalling regulation instead.

EF-P was also found to be important for the synthesis of other carbohydrate transporters. The *efp* deletion mutant shows growth impairment depending on the available carbohydrates, and the severity of the growth defects is correlated with the efficacy of the polyproline stalling motifs that occur in the sequences that code for these proteins.

Polyproline motifs are frequently found in protein-protein interaction sites. In EII<sup>Glc</sup>, the EF-P-dependent polyproline motif is predicted to be located in a transmembrane domain of the EIIC subunit of EII<sup>Glc</sup>, which is involved in dimer formation. Avoiding a bottleneck in EII<sup>Glc</sup> production by replacing one or the two prolines of this motif completely inhibited growth of the corresponding *C. glutamicum* mutants on glucose as sole carbon source. An unbiased semi-random mutagenesis approach further confirmed that the consecutive prolines are essential for the function of EII<sup>Glc</sup>. Previous studies on the role of polyproline motifs in membrane-integrated proteins have focused on the *E. coli* acid stress receptor CadC (Ude et al., 2013) and the osmosensor EnvZ (Motz and Jung, 2018). CadC has a strong polyproline motif that fine-tunes its copy number (Ude et al., 2013). A CadC variant in which the triproline motif is replaced by a pair of alanines is characterized by 3-fold higher copy number and a less sensitive stress response. On the other hand, the polyproline motif in EnvZ did not affect receptor copy number, but was found to be essential for dimerization and interaction with the modulator MzrA (Motz and Jung, 2018). Here, we

propose that the polyproline motif in *C. glutamicum* EII<sup>Glc</sup> has a dual function: it is essential for permease activity, but also fine-tunes the amount of the transporter that is produced.

Overall, our study shows that EF-P plays an important role in the translation of carbohydrate transporters in *C. glutamicum*. Regulation at the translational level might be considered in the process of strain optimization, especially when aiming to increase carbohydrate uptake rates.

## EXPERIMENTAL PROCEDURES

**Nucleotides, plasmids and bacterial strain construction.** DNA sequences, plasmids and strains used in this study are listed in Supplementary Tables S1-S3. Genomic DNA was purified from *C. glutamicum* ATCC 13032 using Nucleospin Microbial DNA columns (Macherey-Nagel). For cloning, Q5 DNA polymerase and restriction enzymes from New England Biolabs (NEB) were used according to the manufacturer's protocols. Deletion and gene fusion strains were constructed by allelic recombination with the pK19mobSacB vectors listed in Table S2 and identified by SacB counterselection. Codon replacements were introduced by overlap-extension PCR using mismatched primers (Ho et al., 1989). Primers containing random codons at positions 235 or 236 of *ptsG* were used to construct a *ptsG* library in the self-replicating vector pEKEx2.

**Growth conditions.** Brain-heart infusion medium (BHI – Becton Dickinson) 37g L<sup>-1</sup> was used as the standard complex medium for growth of *C. glutamicum*. Cells were also grown in chemically defined CGXII media supplemented with 2% (w/v) of the specified carbon source (Keilhauer et al., 1993). In general, cells were cultivated in 100 mL-baffled flasks filled with 25 mL with a starting OD<sub>600</sub> of 1 at 30°C on a rotatory shaker. Overnight cultures were done in BHI medium, and cells were washed in phosphate-buffered saline (PBS; pH 7.4) before inoculation. In some cases (Figure 4) growth experiments were done in 96-well plates incubated at 30°C and 220 rpm. Cells were freshly transformed to avoid formation of suppressor mutants.

**Single-cell fluorescence microscopy analysis.** For quantification of mNG-EII<sup>Glc</sup> and GntR2-mCherry, cells were grown in rich BHI medium supplemented with 2% (w/v) glucose until OD<sub>600</sub> = 2. Cells were then collected, washed in ice-cold phosphate-buffered saline (PBS; pH 7.4), placed on an agarose pad (1% w/v agarose in PBS) and covered with a coverslip. Fluorescence images of cells producing mNG-EII<sup>Glc</sup> were taken on a Delta Vision Elite (GE Healthcare, Applied Precision) equipped with Insight SSI illumination, X4 laser module and a Cool Snap HQ2 CCD camera. Exposure times were limited to 2,000 ms. Images of cells

expressing GntR2-mCherry were taken on a Leica microscope DMI6000B equipped with a DFC365 Fx camera (Leica) and a 300-ms exposure time was used. Excitation and emission filters were selected as appropriate for the relevant fluorophore: 460/512 for mNeonGreen and 546/605 for mCherry. The control experiments of non-fused mNeonGreen or mCherry overexpression in the wild-type and *efp*<sup>-</sup> background were performed with cells cultivated in rich BHI medium supplemented with 0.5 mM IPTG until OD<sub>600</sub> = 2 and fluorescence was assessed with a DFC365 Fx camera (Leica) and 300-ms or 60 ms exposure time, respectively. At least 300 cells per condition were analyzed. Digital images were analyzed using Fiji (Schindelin et al., 2012).

**RT-qPCR analysis.** The RNA used for reverse transcription qPCR was isolated using the phenol-chloroform-isoamyl alcohol (PCI) protocol (Russell and Sambrook, 2001) with modifications. 50 mg of bacterial pellet was washed in 1 mL of ice-cold AE buffer (20 mM sodium acetate buffer, pH 5.2, 1 mM EDTA) and resuspended in 500  $\mu$ L of the same buffer. Then 500  $\mu$ L of pre-warmed PCI for RNA extraction (Roth, X985) and 25  $\mu$ L of 10% (w/v) SDS were added and the mixture was incubated for 5 min at 60°C under vigorous agitation. Samples were cooled for 2 h on ice and centrifuged for 1 h at 16,000g. The supernatant was transferred to phase-lock tubes (Quanta), and 1.0 volume of PCI and 0.1 volume of 3 M sodium acetate (pH 5.2) were added before centrifugation for 15 min. The supernatant was collected, mixed with 2.3 volumes of ethanol and placed in a -80°C freezer overnight. After centrifugation at 16,000g for 1 h, the supernatant was discarded and the pellet was washed twice with 70% (v/v) ethanol, dried and resuspended in 100  $\mu$ L of RNase-free water. A 1- $\mu$ g aliquot of the isolated total RNA was converted to cDNA with the iScript Advanced Script (Bio-Rad) according to the manufacturer's protocol. Samples were mixed with SsoAdvanced Univ SYBR Green Supermix (Bio-Rad), dispensed in triplicate onto a 96-well PCR plate (Bio-Rad) and subjected to qPCR in a Bio-Rad CFX real-time cycler. Evaluation of the data obtained was performed according to the  $\Delta\Delta$ Ct method, using 16S rRNA and *dnaE* as internal references (Schmittgen and Livak, 2008).

**Purification of active post-translationally modified *E. coli* EF-P.** *E. coli* MG1655 cells that had been transformed with pBAD33 encoding EF-P-6xHis, EpmA and EpmB were grown to OD<sub>600</sub> 2, induced with 0.2% (w/v) arabinose, and incubated overnight at 18°C under constant aeration. Cells were then collected, resuspended in lysis buffer [25 mM HEPES-KOH pH 8, 125 mM NaCl, 25 mM KCl, 10% (v/v) glycerol] and lysed using a high-pressure system (Constant Systems). The cytosolic protein fraction was obtained by centrifugation of the lysate, and EF-P was purified on a Ni<sup>2+</sup>-nitrilotriacetic acid (NTA) resin (Qiagen). After washing with lysis buffer supplemented with 20 mM imidazole, bound EF-P was eluted with 200 mM imidazole in the same buffer.

**In vitro translation of EII<sup>Glc</sup>.** The PURExpress *In vitro* Protein Synthesis Kit (NEB, E6800) was used for in vitro translation of EII<sup>Glc</sup>, with the following modifications. To avoid protein aggregation, the reaction mix was supplemented with 1 mM arginine (pH 7.0) and 1 mM β-mercaptoethanol. Purified post-translationally modified *E. coli* EF-P was added at 1 μM concentration. The same amount of lysis buffer was added to the negative control. The tubes were incubated for 3 min at 37°C prior to the addition of DNA. To start the reaction, 200 ng of DNA coding for FT-EII<sup>Glc</sup>-FT was added. Samples were taken at 0, 15, 30 and 45 min, and the translation reaction was stopped by homogenizing the sample in a stop-solution containing 0.1 M kanamycin, 8 M urea, 400 mM arginine (pH 7.0) and 10 mM β-mercaptoethanol. Samples (2.5 μL) were then loaded onto a SDS-polyacrylamide gel (Laemmli, 1970) to fractionate the proteins by size, and further analyzed after Western blotting.

**Western blot.** The wet-transfer method was used to transfer the proteins from SDS-polyacrylamide gels to nitrocellulose membranes (Amersham, GE Healthcare). Primary and secondary antibodies were diluted in TBS [10 mM Tris/HCl pH 7.5, 150 mM NaCl] supplemented with 3% (w/v) bovine serum albumin, and used in the following dilutions: 1:1,000 for monoclonal mouse anti-mNeonGreen antibodies (Chromotek, 32F6), 1:4,000 for polyclonal rabbit antibodies against *E. coli* EF-P (Eurogentec), 1:10,000 for monoclonal mouse anti-Flag antibodies (Sigma, A8592), 1:20,000 for rabbit anti-6xHis antibody. The secondary, fluorescent antibodies employed – goat anti-mouse IgG antibodies (Abcam, ab216776) and goat anti-rabbit antibodies (Abcam, ab216773) – were diluted 1:20,000 prior to use. Intermediate washing steps were carried out in TBS-TT buffer [10 mM Tris/HCl pH 7.5, 500 mM NaCl, 0.05% (v/v) Tween 20, 0.2% (v/v) Triton X100]. Images were taken using the Odyssey CLx imaging system (LI-COR Biosciences).

**D-glucose-6-<sup>14</sup>C uptake assay.** All uptake measurements were performed as described earlier with minor modifications (Lindner et al., 2011). Cells were grown in BHI medium supplemented with 2% (w/v) glucose to OD<sub>600</sub> 2, harvested by centrifugation, then washed three times in ice-cold CGXII medium (without carbon sources), resuspended to OD<sub>600</sub> = 2 and stored on ice until analyzed. Prior to measurement, 2-mL aliquots of cell culture were incubated for 3 min at 30°C in a water bath. The reaction was started by the addition of 5, 50 or 500 μM D-glucose-6-<sup>14</sup>C (59 mCi/nmol; Sigma, G9899). At 30-sec intervals, 200-μL samples were filtered through glass-fiber filters (Type F, Millipore) and washed twice with 2.5 mL of 100 mM LiCl. The radioactivity in the samples was determined using scintillation fluid (MP Biomedicals) and a scintillation counter (PerkinElmer).

**EII<sup>Glc</sup> tertiary-structure prediction.** The amino acid sequence of the EII<sup>Glc</sup> domain of EII<sup>Glc</sup> was uploaded to the Phyre2 platform using standard parameters (Kelley et al., 2015). The structure was modelled with

100% confidence with a single highest scoring template, PDB 5IWS (*Bacillus cereus* Malt). Output PDB files were visualized using UCSF Chimera v1.14 (Pettersen et al., 2004).

**Construction of the the EIIC phylogenetic tree.** The amino acid sequence of the EIIC domain of *C. glutamicum* EII<sup>Glc</sup> (Uniprot reference Q46072) corresponding to the amino acids from position 117 to 476 was downloaded and the 20.000 most similar sequences identified using Basic Local Alignment Search Tool (BLAST), excluding sequences from uncultured/environmental samples. The data set was reined by deleting partial sequences, hypothetical proteins, sequences that do not contain domain IIC and identical sequences. Data was retrieved against the Uniprot annotated database resulting in 4.218 non redundant sequences. The sequence of *Bacillus cereus* Malt was added for comparison. Protein sequences alignment was performed using MAFFT FFT-NS-2 method (Katoh et al., 2019). Maximal likelihood protein trees were constructed using the software tool RAxML-HPC v.8 (Stamatakis, 2014). Tree display was done using the software tool iTOL v3 (Letunic and Bork, 2016).

#### ACKNOWLEDGMENTS

This work was funded in part by a fellowship awarded to B.P. by the Brazilian Exchange Program “Science Without Borders”. We thank the Deutsche Forschungsgemeinschaft for grants TRR174 (to K.J. and M.B.) and GRK2062 (to K.J.) to financially support this work. We are grateful to Dr. Oliver Goldbeck and Dr. Gerd Seibold who provided us with the strain *C. glutamicum*  $\Delta ptsG \Delta iolT1 \Delta iolT2$ . We thank Manuela Grafemeyer for providing strains *C. glutamicum*/pEKEX2 and *C. glutamicum*/pEKEX2-mNG.

#### AUTHOR CONTRIBUTIONS

B.P., D.P.P., M.B. and K.J. designed the experiments. B.P. and G.B.M. constructed strains and plasmids. B.P., D.P.P., and L.G. performed the experiments. B.P., D.P.P. and K.J. wrote the manuscript. K.J. supervised the project.

#### REFERENCES

- BECKER, J., GIESELMANN, G., HOFFMANN, S. L. & WITTMANN, C. 2018. *Corynebacterium glutamicum* for Sustainable Bioproduction: From Metabolic Physiology to Systems Metabolic Engineering. *Adv Biochem Eng Biotechnol*, 162, 217-263.
- BRÜHL, N. 2015. Charakterisierung des Fructoseexports in *Corynebacterium glutamicum*. *Dissertation, Universität zu Köln*.
- DEUTSCHER, J., AKE, F. M., DERKAOUI, M., ZEBRE, A. C., CAO, T. N., BOURAOUI, H., KENTACHE, T., MOKHTARI, A., MILOHANIC, E. & JOYET, P. 2014. The bacterial phosphoenolpyruvate:carbohydrate phosphotransferase system: regulation by protein phosphorylation and phosphorylation-dependent protein-protein interactions. *Microbiol Mol Biol Rev*, 78, 231-56.
- DOERFEL, L. K., WOHLGEMUTH, I., KOTHE, C., PESKE, F., URLAUB, H. & RODNINA, M. V. 2013. EF-P is essential for rapid synthesis of proteins containing consecutive proline residues. *Science*, 339, 85-8.
- EGGELING, L. & BOTT, M. 2015. A giant market and a powerful metabolism: L-lysine provided by *Corynebacterium glutamicum*. *Appl Microbiol Biotechnol*, 99, 3387-94.
- ELGAMAL, S., KATZ, A., HERSCH, S. J., NEWSOM, D., WHITE, P., NAVARRE, W. W. & IBBA, M. 2014. EF-P dependent pauses integrate proximal and distal signals during translation. *PLoS Genet*, 10, e1004553.
- ENGELS, V. & WENDISCH, V. F. 2007. The DeoR-type regulator SugR represses expression of *ptsG* in *Corynebacterium glutamicum*. *J Bacteriol*, 189, 2955-66.
- FRUNZKE, J., ENGELS, V., HASENBEIN, S., GATGENS, C. & BOTT, M. 2008. Co-ordinated regulation of gluconate catabolism and glucose uptake in *Corynebacterium glutamicum* by two functionally equivalent transcriptional regulators, GntR1 and GntR2. *Mol Microbiol*, 67, 305-22.
- GAIGALAT, L., SCHLUTER, J. P., HARTMANN, M., MORMANN, S., TAUCH, A., PUHLER, A. & KALINOWSKI, J. 2007. The DeoR-type transcriptional regulator SugR acts as a repressor for genes encoding the phosphoenolpyruvate:sugar phosphotransferase system (PTS) in *Corynebacterium glutamicum*. *BMC Mol Biol*, 8, 104.
- GORKE, B. & STULKE, J. 2008. Carbon catabolite repression in bacteria: many ways to make the most out of nutrients. *Nat Rev Microbiol*, 6, 613-24.
- GUTIERREZ, E., SHIN, B. S., WOOLSTENHULME, C. J., KIM, J. R., SAINI, P., BUSKIRK, A. R. & DEVER, T. E. 2013. eIF5A promotes translation of polyproline motifs. *Mol Cell*, 51, 35-45.

- HASEGAWA, S., TANAKA, Y., SUDA, M., JOJIMA, T. & INUI, M. 2017. Enhanced Glucose Consumption and Organic Acid Production by Engineered *Corynebacterium glutamicum* Based on Analysis of a *pfkB1* Deletion Mutant. *Appl Environ Microbiol*, 83.
- HEIDER, S. A. & WENDISCH, V. F. 2015. Engineering microbial cell factories: Metabolic engineering of *Corynebacterium glutamicum* with a focus on non-natural products. *Biotechnol J*, 10, 1170-84.
- HENKE, N. A., WIEBE, D., PEREZ-GARCIA, F., PETERS-WENDISCH, P. & WENDISCH, V. F. 2018. Coproduction of cell-bound and secreted value-added compounds: Simultaneous production of carotenoids and amino acids by *Corynebacterium glutamicum*. *Bioresour Technol*, 247, 744-752.
- HERSCH, S. J., WANG, M., ZOU, S. B., MOON, K. M., FOSTER, L. J., IBBA, M. & NAVARRE, W. W. 2013. Divergent protein motifs direct elongation factor P-mediated translational regulation in *Salmonella enterica* and *Escherichia coli*. *mBio*, 4, e00180-13.
- HO, S. N., HUNT, H. D., HORTON, R. M., PULLEN, J. K. & PEASE, L. R. 1989. Site-directed mutagenesis by overlap extension using the polymerase chain reaction. *Gene*, 77, 51-9.
- HUMMELS, K. R. & KEARNS, D. B. 2019. Suppressor mutations in ribosomal proteins and FliY restore *Bacillus subtilis* swarming motility in the absence of EF-P. *PLoS Genet*, 15, e1008179
- HUMMELS, K. R., WITZKY, A., RAJKOVIC, A., TOLLERSON, R., 2ND, JONES, L. A., IBBA, M. & KEARNS, D. B. 2017. Carbonyl reduction by Ymfl in *Bacillus subtilis* prevents accumulation of an inhibitory EF-P modification state. *Mol Microbiol*, 106, 236-251.
- IKEDA, M. 2012. Sugar transport systems in *Corynebacterium glutamicum*: features and applications to strain development. *Appl Microbiol Biotechnol*, 96, 1191-200.
- IKEDA, M., MIZUNO, Y., AWANE, S., HAYASHI, M., MITSUHASHI, S. & TAKENO, S. 2011. Identification and application of a different glucose uptake system that functions as an alternative to the phosphotransferase system in *Corynebacterium glutamicum*. *Appl Microbiol Biotechnol*, 90, 1443-51.
- JOJIMA, T., NOBURYU, R., SASAKI, M., TAJIMA, T., SUDA, M., YUKAWA, H. & INUI, M. 2015. Metabolic engineering for improved production of ethanol by *Corynebacterium glutamicum*. *Appl Microbiol Biotechnol*, 99, 1165-72.
- KALINOWSKI, J., BATHE, B., BARTELS, D., BISCHOFF, N., BOTT, M., BURKOVSKI, A., DUSCH, N., EGGELING, L., EIKMANN, B. J., GAIGALAT, L., GOESMANN, A., HARTMANN, M., HUTHMACHER, K., KRAMER, R., LINKE, B., MCHARDY, A. C., MEYER, F., MOCKEL, B., PFEFFERLE, W., PUHLER, A., REY, D. A., RUCKERT, C., RUPP, O., SAHM, H., WENDISCH, V. F., WIEGRABE, I. & TAUCH, A. 2003. The complete *Corynebacterium glutamicum* ATCC 13032 genome sequence and its impact on the production of L-aspartate-derived amino acids and vitamins. *J Biotechnol*, 104, 5-25.

- KALLSCHEUER, N., CLASSEN, T., DREPPER, T. & MARIENHAGEN, J. 2019. Production of plant metabolites with applications in the food industry using engineered microorganisms. *Curr Opin Biotechnol*, 56, 7-17.
- KALLSCHEUER, N., VOGT, M., BOTT, M. & MARIENHAGEN, J. 2017. Functional expression of plant-derived O-methyltransferase, flavanone 3-hydroxylase, and flavonol synthase in *Corynebacterium glutamicum* for production of pterostilbene, kaempferol, and quercetin. *J Biotechnol*, 258, 190-196.
- KALLSCHEUER, N., VOGT, M., STENZEL, A., GATGENS, J., BOTT, M. & MARIENHAGEN, J. 2016. Construction of a *Corynebacterium glutamicum* platform strain for the production of stilbenes and (2S)-flavanones. *Metab Eng*, 38, 47-55.
- KATOH, K., ROZEWICKI, J. & YAMADA, K. D. 2019. MAFFT online service: multiple sequence alignment, interactive sequence choice and visualization. *Brief Bioinform*, 20, 1160-1166.
- KEILHAUER, C., EGGELING, L. & SAHM, H. 1993. Isoleucine synthesis in *Corynebacterium glutamicum*: molecular analysis of the *ilvB-ilvN-ilvC* operon. *J Bacteriol*, 175, 5595-603.
- KELLEY, L. A., MEZULIS, S., YATES, C. M., WASS, M. N. & STERNBERG, M. J. 2015. The Phyre2 web portal for protein modeling, prediction and analysis. *Nat Protoc*, 10, 845-58.
- KOGURE, T. & INUI, M. 2018. Recent advances in metabolic engineering of *Corynebacterium glutamicum* for bioproduction of value-added aromatic chemicals and natural products. *Appl Microbiol Biotechnol*, 102, 8685-8705.
- KRAUSE, F. S., HENRICH, A., BLOMBACH, B., KRAMER, R., EIKMANNNS, B. J. & SEIBOLD, G. M. 2010. Increased glucose utilization in *Corynebacterium glutamicum* by use of maltose, and its application for the improvement of L-valine productivity. *Appl Environ Microbiol*, 76, 370-4.
- LAEMMLI, U. K. 1970. Cleavage of structural proteins during the assembly of the head of bacteriophage T4. *Nature*, 227, 680-5.
- LASSAK, J., KEILHAUER, E. C., FURST, M., WUICHET, K., GODEKE, J., STAROSTA, A. L., CHEN, J. M., SOGAARD-ANDERSEN, L., ROHR, J., WILSON, D. N., HAUSSLER, S., MANN, M. & JUNG, K. 2015. Arginine-rhamnosylation as new strategy to activate translation elongation factor P. *Nat Chem Biol*, 11, 266-70.
- LETUNIC, I. & BORK, P. 2016. Interactive tree of life (iTOL) v3: an online tool for the display and annotation of phylogenetic and other trees. *Nucleic Acids Res*, 44, W242-5.
- LINDNER, S. N., PETROV, D. P., HAGMANN, C. T., HENRICH, A., KRAMER, R., EIKMANNNS, B. J., WENDISCH, V. F. & SEIBOLD, G. M. 2013. Phosphotransferase system-mediated glucose uptake is repressed in

- phosphoglucosyltransferase-deficient *Corynebacterium glutamicum* strains. *Appl Environ Microbiol*, 79, 2588-95.
- LINDNER, S. N., SEIBOLD, G. M., HENRICH, A., KRAMER, R. & WENDISCH, V. F. 2011. Phosphotransferase system-independent glucose utilization in *Corynebacterium glutamicum* by inositol permeases and glucokinases. *Appl Environ Microbiol*, 77, 3571-81.
- MAKI, K., UNO, K., MORITA, T. & AIBA, H. 2008. RNA, but not protein partners, is directly responsible for translational silencing by a bacterial Hfq-binding small RNA. *Proc Natl Acad Sci U S A*, 105, 10332-7.
- MARTINS, G. B., GIACOMELLI, G., GOLDBECK, O., SEIBOLD, G. M. & BRAMKAMP, M. 2019. Substrate-dependent cluster density dynamics of *Corynebacterium glutamicum* phosphotransferase system permeases. *Mol Microbiol*, 111, 1335-1354.
- MCCOY, J. G., REN, Z., STANEVICH, V., LEE, J., MITRA, S., LEVIN, E. J., POGET, S., QUICK, M., IM, W. & ZHOU, M. 2016. The Structure of a Sugar Transporter of the Glucose EIIc Superfamily Provides Insight into the Elevator Mechanism of Membrane Transport. *Structure*, 24, 956-64.
- MEISWINKEL, T. M., GOPINATH, V., LINDNER, S. N., NAMPOOTHIRI, K. M. & WENDISCH, V. F. 2013. Accelerated pentose utilization by *Corynebacterium glutamicum* for accelerated production of lysine, glutamate, ornithine and putrescine. *Microb Biotechnol*, 6, 131-40.
- MOON, M. W., KIM, H. J., OH, T. K., SHIN, C. S., LEE, J. S., KIM, S. J. & LEE, J. K. 2005. Analyses of enzyme II gene mutants for sugar transport and heterologous expression of fructokinase gene in *Corynebacterium glutamicum* ATCC 13032. *FEMS Microbiol Lett*, 244, 259-66.
- MOON, M. W., PARK, S. Y., CHOI, S. K. & LEE, J. K. 2007. The phosphotransferase system of *Corynebacterium glutamicum*: features of sugar transport and carbon regulation. *J Mol Microbiol Biotechnol*, 12, 43-50.
- MORITA, T., MAKI, K. & AIBA, H. 2005. RNase E-based ribonucleoprotein complexes: mechanical basis of mRNA destabilization mediated by bacterial noncoding RNAs. *Genes Dev*, 19, 2176-86.
- MOTZ, M. & JUNG, K. 2018. The role of polyproline motifs in the histidine kinase EnvZ. *PLoS One*, 13, e0199782.
- NGUYEN, T. X., YEN, M. R., BARABOTE, R. D. & SAIER, M. H., JR. 2006. Topological predictions for integral membrane permeases of the phosphoenolpyruvate:sugar phosphotransferase system. *J Mol Microbiol Biotechnol*, 11, 345-60.
- PEIL, L., STAROSTA, A. L., VIRUMAE, K., ATKINSON, G. C., TENSON, T., REMME, J. & WILSON, D. N. 2012. Lys34 of translation elongation factor EF-P is hydroxylated by YfcM. *Nat Chem Biol*, 8, 695-7.

- PETERS-WENDISCH, P., GOTKER, S., HEIDER, S. A., KOMATI REDDY, G., NGUYEN, A. Q., STANSEN, K. C. & WENDISCH, V. F. 2014. Engineering biotin prototrophic *Corynebacterium glutamicum* strains for amino acid, diamine and carotenoid production. *J Biotechnol*, 192 Pt B, 346-54.
- PETTERSEN, E. F., GODDARD, T. D., HUANG, C. C., COUCH, G. S., GREENBLATT, D. M., MENG, E. C. & FERRIN, T. E. 2004. UCSF Chimera--a visualization system for exploratory research and analysis. *J Comput Chem*, 25, 1605-12.
- PFEIFER, E., GATGENS, C., POLEN, T. & FRUNZKE, J. 2017. Adaptive laboratory evolution of *Corynebacterium glutamicum* towards higher growth rates on glucose minimal medium. *Sci Rep*, 7, 16780.
- PINHEIRO, B., SCHEIDLER, C. M., KIELKOWSKI, P., SCHMID, M., FORNE, I., YE, S., REILING, N., TAKANO, E., IMHOF, A., SIEBER, S. A., SCHNEIDER, S. & JUNG, K. 2020. Structure and Function of an Elongation Factor P Subfamily in Actinobacteria. *Cell Rep*, 30, 4332-4342 e5.
- PRUNETTI, L., GRAF, M., BLABY, I. K., PEIL, L., MAKKAY, A. M., STAROSTA, A. L., PAPKE, R. T., OSHIMA, T., WILSON, D. N. & DE CRECY-LAGARD, V. 2016. Deciphering the Translation Initiation Factor 5A Modification Pathway in Halophilic Archaea. *Archaea*, 2016, 7316725.
- QI, F., MOTZ, M., JUNG, K., LASSAK, J. & FRISHMAN, D. 2018. Evolutionary analysis of polyproline motifs in *Escherichia coli* reveals their regulatory role in translation. *PLoS Comput Biol*, 14, e1005987.
- ROY, H., ZOU, S. B., BULLWINKLE, T. J., WOLFE, B. S., GILREATH, M. S., FORSYTH, C. J., NAVARRE, W. W. & IBBA, M. 2011. The tRNA synthetase paralog PoxA modifies elongation factor-P with (R)-beta-lysine. *Nat Chem Biol*, 7, 667-9.
- RUSSELL, D. W. & SAMBROOK, J. 2001. *Molecular cloning: a laboratory manual*, Cold Spring Harbor Laboratory Cold Spring Harbor, NY.
- SANCHEZ, S., RODRIGUEZ-SANOJA, R., RAMOS, A. & DEMAIN, A. L. 2017. Our microbes not only produce antibiotics, they also overproduce amino acids. *J Antibiot (Tokyo)*.
- SCHINDELIN, J., ARGANDA-CARRERAS, I., FRISE, E., KAYNIG, V., LONGAIR, M., PIETZSCH, T., PREIBISCH, S., RUEDEN, C., SAALFELD, S., SCHMID, B., TINEVEZ, J. Y., WHITE, D. J., HARTENSTEIN, V., ELICEIRI, K., TOMANCAK, P. & CARDONA, A. 2012. Fiji: an open-source platform for biological-image analysis. *Nat Methods*, 9, 676-82.
- SCHMITTGEN, T. D. & LIVAK, K. J. 2008. Analyzing real-time PCR data by the comparative C(T) method. *Nat Protoc*, 3, 1101-8.
- SIEBERT, D. & WENDISCH, V. F. 2015. Metabolic pathway engineering for production of 1,2-propanediol and 1-propanol by *Corynebacterium glutamicum*. *Biotechnol Biofuels*, 8, 91.

- STAMATAKIS, A. 2014. RAxML version 8: a tool for phylogenetic analysis and post-analysis of large phylogenies. *Bioinformatics*, 30, 1312-3.
- STAROSTA, A. L., LASSAK, J., PEIL, L., ATKINSON, G. C., VIRUMAE, K., TENSION, T., REMME, J., JUNG, K. & WILSON, D. N. 2014a. Translational stalling at polyproline stretches is modulated by the sequence context upstream of the stall site. *Nucleic Acids Res*, 42, 10711-9.
- STAROSTA, A. L., LASSAK, J., PEIL, L., ATKINSON, G. C., WOOLSTENHULME, C. J., VIRUMAE, K., BUSKIRK, A., TENSION, T., REMME, J., JUNG, K. & WILSON, D. N. 2014b. A conserved proline triplet in Val-tRNA synthetase and the origin of elongation factor P. *Cell Rep*, 9, 476-83.
- TANAKA, Y., OKAI, N., TERAMOTO, H., INUI, M. & YUKAWA, H. 2008a. Regulation of the expression of phosphoenolpyruvate: carbohydrate phosphotransferase system (PTS) genes in *Corynebacterium glutamicum*. *Microbiology*, 154, 264-74.
- TANAKA, Y., TAKEMOTO, N., ITO, T., TERAMOTO, H., YUKAWA, H. & INUI, M. 2014. Genome-wide analysis of the role of global transcriptional regulator GntR1 in *Corynebacterium glutamicum*. *J Bacteriol*, 196, 3249-58.
- TANAKA, Y., TERAMOTO, H., INUI, M. & YUKAWA, H. 2008b. Regulation of expression of general components of the phosphoenolpyruvate: carbohydrate phosphotransferase system (PTS) by the global regulator SugR in *Corynebacterium glutamicum*. *Appl Microbiol Biotechnol*, 78, 309-18.
- UDE, S., LASSAK, J., STAROSTA, A. L., KRAXENBERGER, T., WILSON, D. N. & JUNG, K. 2013. Translation elongation factor EF-P alleviates ribosome stalling at polyproline stretches. *Science*, 339, 82-5.
- WANG, C., CAI, H., ZHOU, Z., ZHANG, K., CHEN, Z., CHEN, Y., WAN, H. & OUYANG, P. 2014. Investigation of *ptsG* gene in response to xylose utilization in *Corynebacterium glutamicum*. *J Ind Microbiol Biotechnol*, 41, 1249-58.
- WANG, Z., LIU, J., CHEN, L., ZENG, A. P., SOLEM, C. & JENSEN, P. R. 2018. Alterations in the transcription factors GntR1 and RamA enhance the growth and central metabolism of *Corynebacterium glutamicum*. *Metab Eng*, 48, 1-12.
- WENDISCH, V. F., BRITO, L. F., GIL LOPEZ, M., HENNIG, G., PFEIFENSCHNEIDER, J., SGOBBA, E. & VELDMANN, K. H. 2016a. The flexible feedstock concept in Industrial Biotechnology: Metabolic engineering of *Escherichia coli*, *Corynebacterium glutamicum*, *Pseudomonas*, *Bacillus* and yeast strains for access to alternative carbon sources. *J Biotechnol*, 234, 139-157.
- WENDISCH, V. F., DE GRAAF, A. A., SAHM, H. & EIKMANN, B. J. 2000. Quantitative determination of metabolic fluxes during cointilization of two carbon sources: comparative analyses with *Corynebacterium glutamicum* during growth on acetate and/or glucose. *J Bacteriol*, 182, 3088-96.

WENDISCH, V. F., JORGE, J. M. P., PEREZ-GARCIA, F. & SGOBBA, E. 2016b. Updates on industrial production of amino acids using *Corynebacterium glutamicum*. *World J Microbiol Biotechnol*, 32, 105.

WOOLSTENHULME, C. J., GUYDOSH, N. R., GREEN, R. & BUSKIRK, A. R. 2015. High-precision analysis of translational pausing by ribosome profiling in bacteria lacking EFP. *Cell Rep*, 11, 13-21.

XIAO, S., XU, J., CHEN, X., LI, X., ZHANG, Y. & YUAN, Z. 2016. 3-Methyl-1-butanol Biosynthesis in an Engineered *Corynebacterium glutamicum*. *Mol Biotechnol*, 58, 311-8.

XU, J., ZHANG, J., LIU, D. & ZHANG, W. 2016. Increased glucose utilization and cell growth of *Corynebacterium glutamicum* by modifying the glucose-specific phosphotransferase system (PTS(Glc)) genes. *Can J Microbiol*, 62, 983-992.

YANAGISAWA, T., SUMIDA, T., ISHII, R., TAKEMOTO, C. & YOKOYAMA, S. 2010. A paralog of lysyl-tRNA synthetase aminoacylates a conserved lysine residue in translation elongation factor P. *Nat Struct Mol Biol*, 17, 1136-43.

## TABLES

**Table 1** – Polyproline motifs found in proteins involved in carbohydrate transport and metabolism in *C. glutamicum* ATCC 13032. The amino acid context (positions -2, -1 and +1) of each motif is shown.

Name	Reference	Motif sequence	Polyproline position	Predicted Stalling Strength (Qi et al., 2018)
EII <sup>Glc</sup>	Q46072	VFPPPL	235/236	Moderate
EII <sup>Fru</sup>	Q8NP80	MVPPI	479/480	Weak
EII <sup>Scr</sup>	Q8NMD6	SFPPI	328/329	Weak
GntP	Q79VC5	FVPPH	166/167	Weak
PfkB	Q8NP81	SLPPG	139/140	Weak

ScrB	Q8NMD5	VTPPQ	20/21	Weak
GntR2	Q8NPU3	MAPPI	187/188	Moderate
FruR	Q8NP82	TSPPR/GMPPE	67/68 and 79/80	Weak

## FIGURE LEGENDS

**Figure 1** – Schematic depictions of the domain structures of PTS systems in *C. glutamicum*. Their substrates, metabolic contexts and transcriptional regulators. The level of shading indicates the relative strengths of the polyproline motifs they contain (listed in Table 1). Fru fructose, Suc sucrose, Glu glucose, Gnt gluconate, Rib ribose, PTS phosphoenolpyruvate-dependent sugar phosphotransferase system. EII<sup>Fru</sup> fructose-specific phosphotransferase system, EII<sup>Suc</sup> sucrose-specific phosphotransferase system, EII<sup>Glc</sup> glucose-specific phosphotransferase system (subunits A, B and C). GntP gluconate permease, ACBDRib ribose specific ATP-binding cassette transporter for D-ribose, F1P fructose-1,6-bisphosphate, F6P fructose-6-phosphate, S6P sucrose-6-phosphate, G6P glucose-6-phosphate, Gnt6P 6-phosphogluconate, R5P ribose-5-phosphate, PfkB fructose-1-phosphate kinase, PfkA 6-phosphofructokinase, Fbp fructose-1,6-bisphosphatase, ScrB sucrose-6-phosphate hydrolase, Pgi phosphoglucose isomerase, Glk glucokinase, PpgK polyphosphate dependent glucokinase, GntK gluconate kinase, RbsK1 ribokinase 1, RbsK2 ribokinase 2. HPr and EI, the heat-stable phosphocarrier protein and enzyme I, are general energy-coupling proteins of the phosphoenolpyruvate-dependent phosphotransferase systems (PTS). HPr and EI are encoded respectively by *ptsH* and *ptsI*. Question marks indicate the transport of certain carbohydrates through unknown or unspecific transporters.

**Figure 2** – Typical growth curves of wild-type *C. glutamicum* ATCC 13032 (brown dots), the *efp* deletion mutant (red dots) and the complemented mutant with *efp in trans* (gray dots). Cells were grown in chemically defined CGXII medium supplemented with the indicated carbon sources (2 % w/v) (A-E) or in complex BHI medium (F) in flasks at 30°C under constant agitation with 180 rpm. Dots represent mean values, and bars depict the standard deviations of the mean of four independent replicates.

**Figure 3** – EII<sup>Glc</sup> translation is dependent on EF-P. (A) Single-cell fluorescence microscopy of *C. glutamicum* cells expressing chromosomally encoded mNG-EII<sup>Glc</sup> in *efp*<sup>+</sup> and *efp*<sup>-</sup> strains. Cells of the untagged parental

strain were used to determine background fluorescence. Exposure time in all cases was 2,000-ms. (B) Distribution of relative mNeonGreen fluorescence intensities of a minimum of 300 *C. glutamicum* cells expressing mNG-EII<sup>Glc</sup> in either the *efp*<sup>+</sup> or the *efp*<sup>-</sup> strain. Black lines indicate the mean fluorescence. The dashed line represents the background fluorescence of the untagged strain. Statistical significance was assessed with the two-tailed t-test. \*\*\*p<0.0001. (C) Quantification of *in vitro*-translated FT-EII<sup>Glc</sup>-FT in the presence and absence of purified EF-P. FT-EII<sup>Glc</sup>-FT was quantified on a Western blot, using the fluorescence-labeled secondary antibody IRDye<sup>®</sup> 680RD. Mean values and standard deviations of three independent experiments are shown. 100% of FT-EII<sup>Glc</sup>-FT production is defined as the production of FT-EII<sup>Glc</sup>-FT PP235/236AA after 45 min incubation in the absence of EF-P. (D) Uptake of radiolabeled D-glucose-6-<sup>14</sup>C by *C. glutamicum efp*<sup>+</sup>, *efp*<sup>-</sup> and *ptsG*<sup>-</sup> strains. Values and standard deviations of five independent experiments are shown.

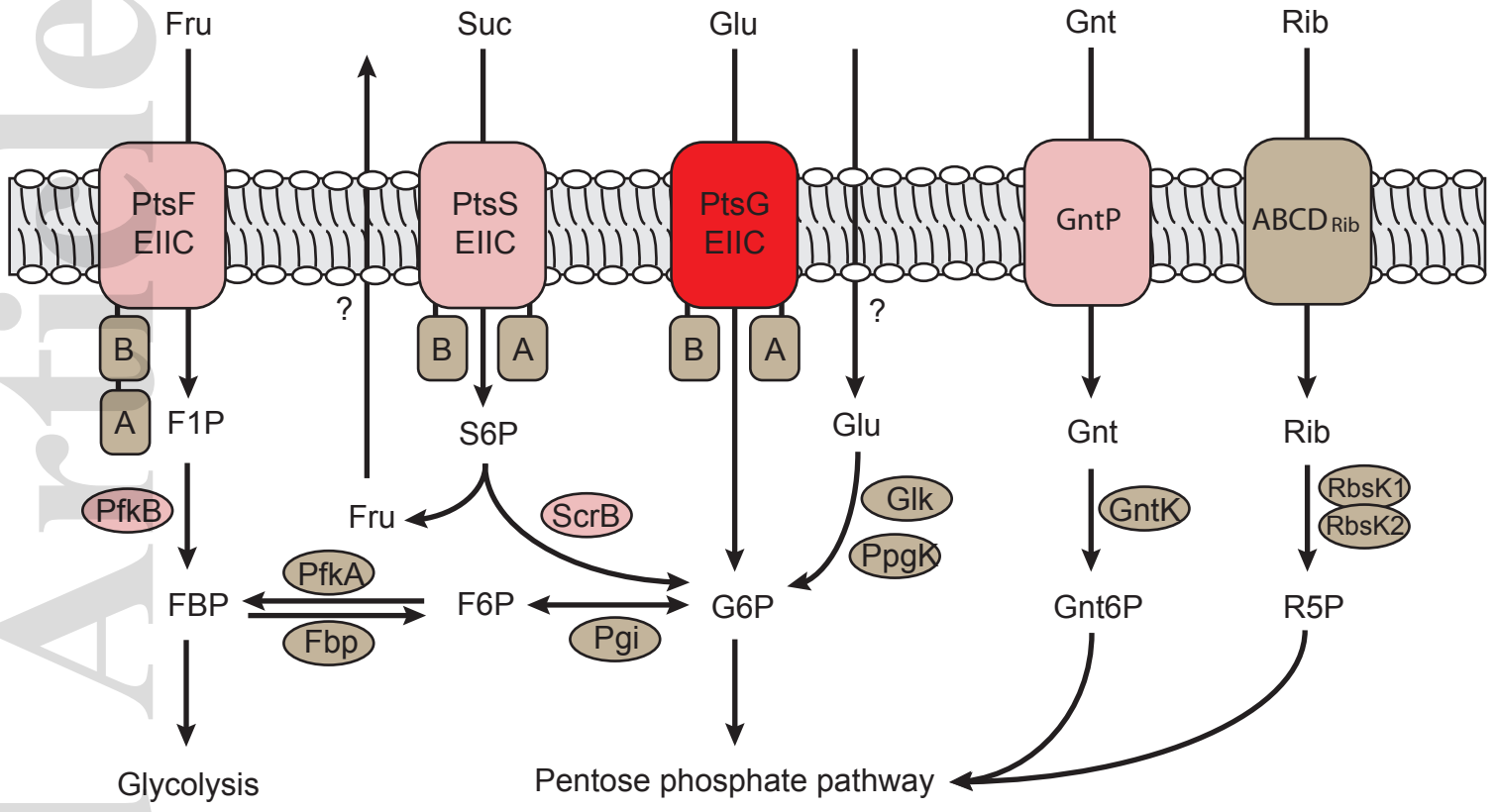
**Figure 4** – The polyproline motif is essential for EII<sup>Glc</sup> function. (A) Growth curves of *C. glutamicum* wild type (brown dots), *C. glutamicum* mNG-EII<sup>Glc</sup> PP235/236AA (green triangles) and *C. glutamicum* mNG-EII<sup>Glc</sup> P236A (blue squares) in complex BHI medium. (B) Growth curves of the same strains as in (A) in chemically defined CGXII medium with glucose as sole carbon source (2% w/v). Cells were cultivated in 96-well microtiter plates (C) Western blot analysis of mNG-EII<sup>Glc</sup> in whole cell lysates of the same *C. glutamicum* strains as in (A). The  $\Delta ptsG$  mutant was included as negative control. (D) Selection of the variants of the EII<sup>Glc</sup> (XPPX motif) obtained after semi-random mutagenesis. (E) 3D structure of *C. glutamicum* EII<sup>Glc</sup> as predicted by Phyre2 (Kelley et al., 2015). Subunit C of EII<sup>Glc</sup> is shown from the side, and the position of the VFPL stalling motif is marked in red. (F) Phylogenetic tree of EIIC permeases from the glucose superfamily, sequences containing polyproline motifs are highlighted in red. The sequence of *B. cereus* MalT was added for comparison.

**Figure 5** – Transcription of *ptsG* is not altered in the  $\Delta efp$  mutant. (A) Single-cell fluorescence microscopy of *C. glutamicum* cells expressing chromosomally encoded GntR2-mCherry in *efp*<sup>+</sup> and *efp*<sup>-</sup> strains. An 800-ms exposure time was used. (B) Distribution of mCherry fluorescence levels detected in samples containing a minimum of 300 cells of each *C. glutamicum* strain. The black lines indicate the mean fluorescence of these cells, and the gray dashed line represents the background fluorescence of the untagged strain. Statistical analysis was done by using two-tailed t test. \*\*\*p<0.0001. (C) Fold change (wild type/ $\Delta efp$ ) of *ptsG* mRNA levels. Cells were cultivated in BHI medium supplemented with 2% (w/v)

glucose to OD<sub>600</sub> 2. Red dots represent the values of four biological replicates, and the mean and standard deviation are indicated.

Accepted Article

FIGURE 1

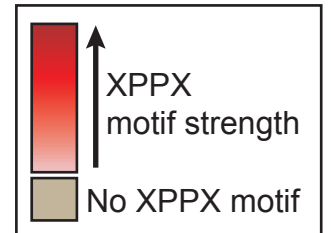


PTS general components



Transcriptional regulators

- SugR ↓ *ptsF*, *ptsS*, *ptsG*, *ptsI* and *ptsH*
- FruR ↓ *ptsF*, *ptsI* and *ptsH*
- GntR1 GntR2 ↑ *ptsG* and *ptsS*, ↓ *gntP* and *gntK*



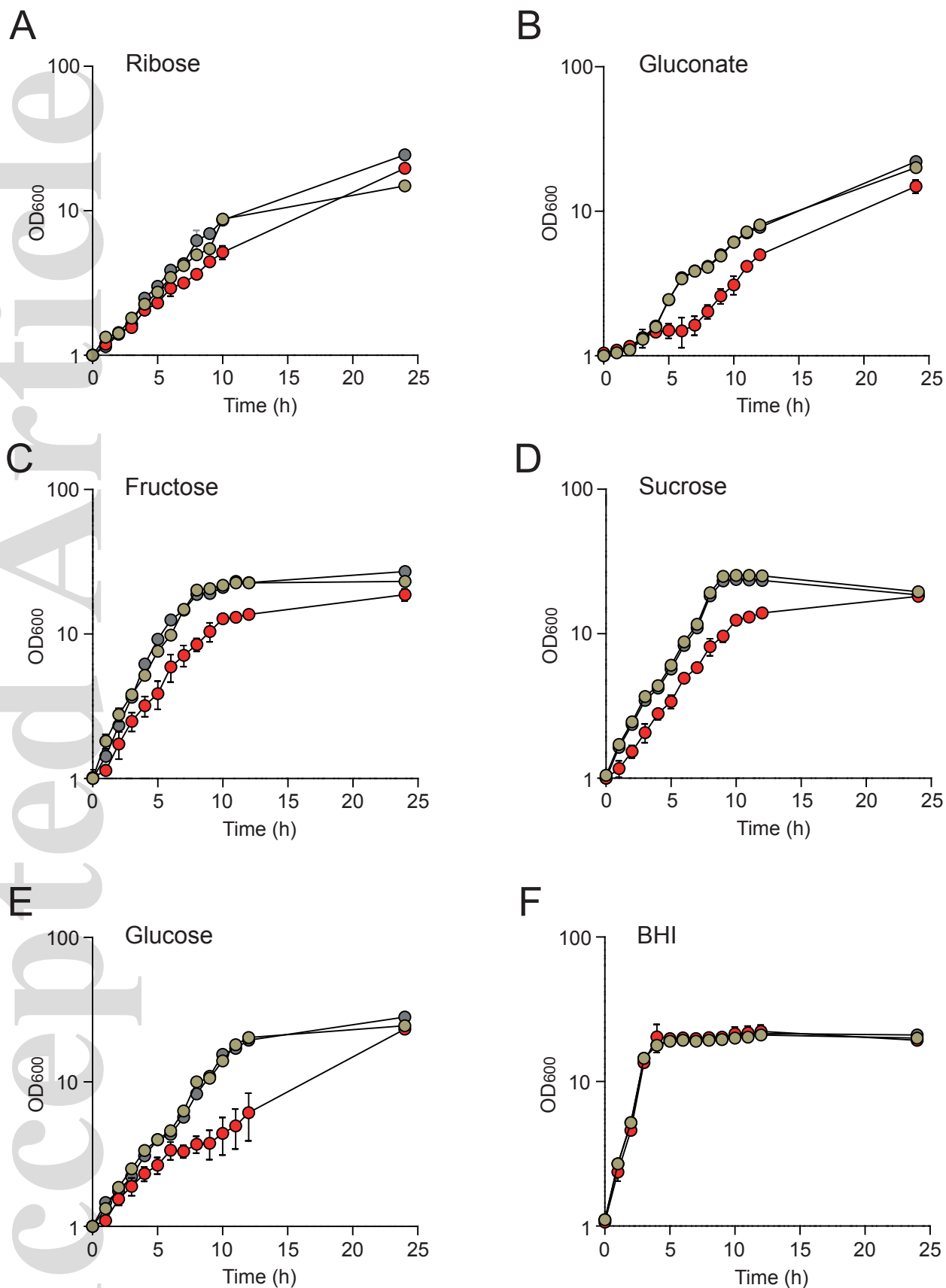


FIGURE 3

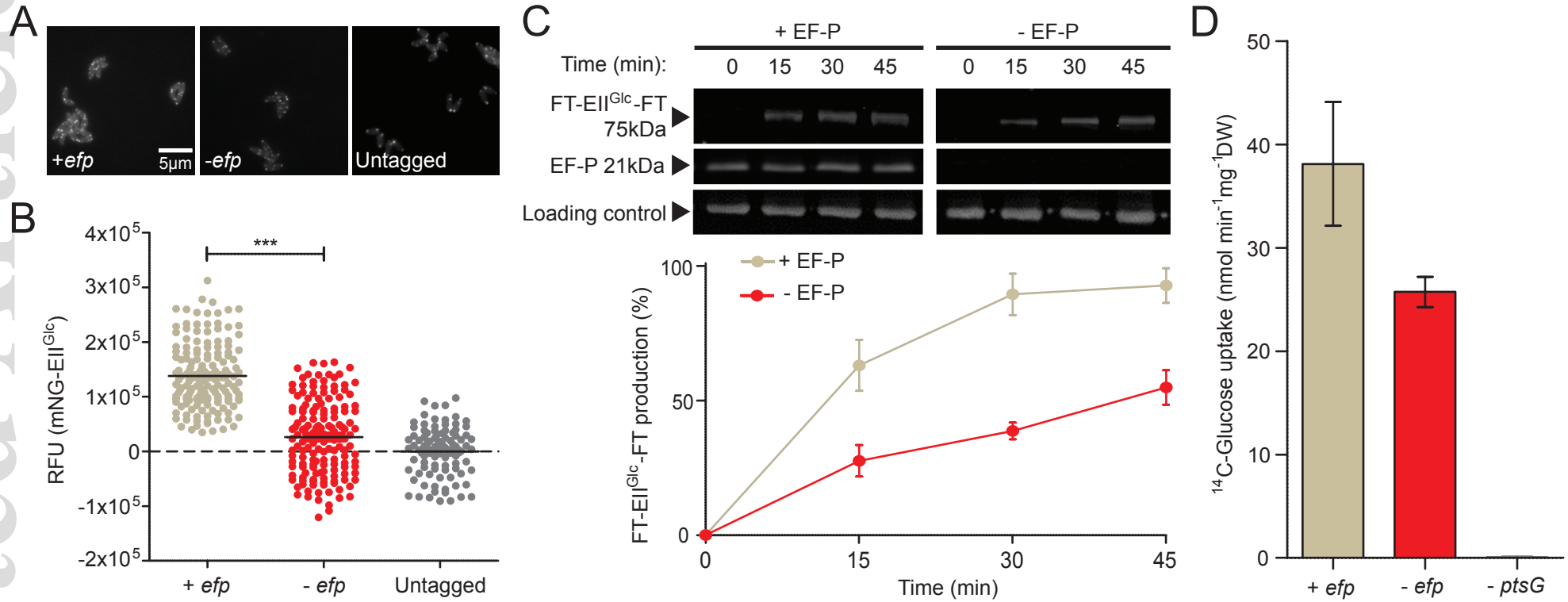


FIGURE 4

mmi\_14618\_f4.pdf

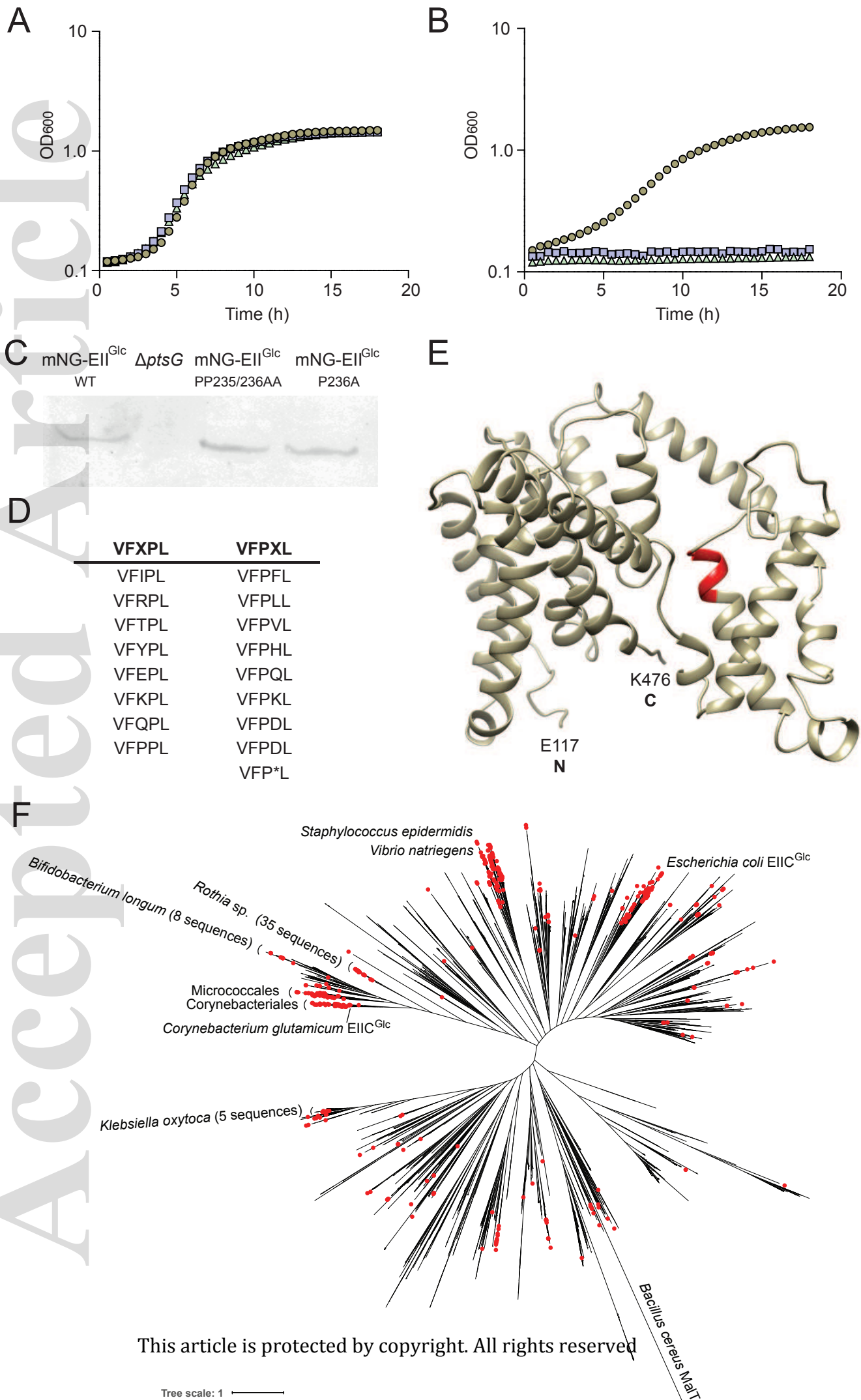


FIGURE 5

